Investigation of the Helical Divertor Function and the Future Plan of a Closed Divertor for Efficient Particle Control in the LHD Plasma Periphery

5.2: INVESTIGATION OF THE HELICAL DIVERTOR FUNCTION AND THE FUTURE PLAN OF A CLOSED DIVERTOR FOR EFFICIENT PARTICLE CONTROL IN THE LHD PLASMA PERIPHERY

*M.SHOJI[a], S.MASUZAKI[a], M.KOBAYASHI[a], M.GOTO[a], T.MORISAKI[a], H.YAMADA[a], A. KOMORI[a] and LHD EXPERIMENT GROUP[a]

[a]*National Institute for Fusion Science, 322-6 Oroshi-cho, Toki, Gifu 509-5292, Japan*

†A.IWAMAE[b], A.SAKAUE[b]

[b]*Department of Mechanical Engineering and Science, Graduate School of Engineering, Kyoto University, Kyoto, 606-8501, Japan*

Total number of pages: 40

Total number of tables: 0

Total number of figures: 14

*E-mail: shoji@LHD.nifs.ac.jp

† present address: *Japan Atomic Energy Agency, 801-1 Mukoyama, Naka, Ibaraki 311-0193, Japan*

ABSTRACT

    The function of the divertor plasmas on the particle control in the plasma periphery is investigated from viewpoints of magnetic field line structures and neutral particle transport in the Large Helical Device. It shows that the particle and heat deposition on the divertor plate arrays are qualitatively explained by the distribution of strike points calculated by magnetic field line tracing including a particle diffusion effect. Control of neutral particle fueling from the divertor plates is a critical issue for sustaining long pulse discharges and achieving Super Dense Core plasmas. The behavior of neutral particles in the plasma periphery has been investigated by H_α emission measurements and a neutral particle transport simulation. It reveals that gas fueling from the toroidally distributed divertor plates heated by protons accelerated by ICRF wave is necessary for explaining measurements in a long pulse discharge, and the spatial profile of the neutral particle density in the plasma periphery in various magnetic configurations is explained by the strike point distribution. Basing on these analyses, a closed helical divertor configuration optimized for the intrinsic magnetic field line structure in the plasma periphery is proposed for efficient particle control and heat load reduction on the divertor plates.

KEWORDS: Helical divertor, Neutral particle transport, Plasma periphery, Large Helical Device, Closed divertor

I. INTRODUCTION

The critical issues for realizing fusion reactors are reduction of heat loads on divertor plates and efficient particle/impurity control in the plasma periphery. Physical understanding of the divertor function is an important task for solving the above two issues. In the Large Helical Device (LHD), divertor plasmas have been fully measured with several plasma diagnostics: Langmuir probes, thermo-couples, visible CCD cameras, an infrared camera, a pyrometer, visible and vacuum ultraviolet spectrometers and so on. Experimental results measured with these plasma diagnostic systems in various magnetic configurations have been investigated by numerical calculations using magnetic field line tracing, a fully three-dimensional plasma fluid code, and neutral particle transport simulation codes, etc.

About ten years plasma discharge operations in the LHD have demonstrated that the neutral particles released from divertor plates significantly affect plasma density control especially in long pulse discharges and high plasma density operation. Suppression of uncontrollable neutral particle fuelling from the divertor plates is essential for sustaining long pulse discharges. Recent plasma discharge experiments demonstrate that peripheral plasma density control is an important issue for achieving super dense core (SDC) plasmas.[1]

A closed helical divertor can contribute to suppression of the peripheral plasma density by controlling the neutral particle fueling from the divertor plates. Detailed understanding of neutral particle transport is essential for optimizing the design of the closed divertor configuration. For these purposes, three-dimensional neutral particle transport simulation codes have been applied to detailed investigation of the effect of

the closed divertor on efficient particle control and reduction of the head load.

In this paper, intrinsic magnetic field line configurations in the LHD plasma periphery are briefly described in the next section. Measurements in two different magnetic configurations and numerical analyses by tracing magnetic field lines are shown in Section 3. The location of neutral particle sources in an ICRF heated long pulse discharge is investigated by a neutral particle transport simulation in Section 4. The effect of magnetic axis swing operation on dispersion of the heat load on divertor plates is described in Section 5, and the analyses of neutral particle transport in the different magnetic configurations by H_α emission measurements and the simulation are shown in Section 6. Optimization of the design of a closed helical divertor by neutral particle transport analyses is explained in the last section.

II. MAGNETIC STRUCTURES IN THE LHD PLASMA PERIPHERY

The LHD is the largest super-conducting helical machine, and its device parameters are: the major radius R=3.9 m, the averaged minor radius a=0.65 m.[2] A helically twisted plasma (ℓ/m=2/10, where ℓ and m are the polarity and the field period, respectively) is formed by the magnetic configuration due to two twisted helical coils and three pairs of circular poloidal coils without plasma currents (no large ELMs and disruptions are induced). The non-axisymmetric magnetic components due to the helical coils produce a three-dimensionally complicated magnetic field line structure (ergodic layer) around the Last Closed Flux Surface (LCFS). The magnetic field lines in the ergodic layer are bundled into four divertor legs on which magnetic field lines are directly connected to water cooled isotropic carbon plates (divertor plates) installed along strike points on the

vacuum vessel. One of the features of the LHD peripheral plasma is high rotational transform in the divertor region. While the connection length of magnetic field lines in the ergodic layer reaches to several km, the connection length on the divertor legs is only a few meter because of the high rotational transform. The radial position of the magnetic axis R_{ax} is controlled by changing the coil currents of the poloidal coils, which also varies the magnetic field line configuration in the ergodic layer and on the divertor legs.

Figure 1 shows the Poincare plots of magnetic field lines in two different magnetic configurations (R_{ax}=3.60 m and 3.75 m) in a plasma horizontally elongated cross section. It indicates that the region of the ergodic layer becomes broad with increase in the radial position of the magnetic axis. While most of the magnetic field lines in the ergodic layer are bundled into two divertor legs in the inboard side of the torus for R_{ax}=3.60 m, most of the magnetic field lines are connected to the outboard side for R_{ax}=3.75 m.

III. PARTICLE AND POWER TRANSPORT IN THE LHD DIVERTOR

In order to achieve efficient particle control and the heat load reduction, understanding of the particle and power transport in the plasma periphery is an important task. The toroidal and poloidal distribution of the particle and power deposition on the divertor plates have been measured with Langmuir probes and thermocouples embedded in divertor plates.[3]

Figure 2(a) illustrates the top view of the equatorial cross section of the LHD vacuum vessel and divertor plate arrays. Single channel H_α emission detectors are mounted on all outer ports for monitoring the toroidal distribution of neutral particles

(hydrogen). The vertical and radial profile of the Hα intensity has been measured with multi-channel Hα emission detector arrays installed in an outer port (1-O) and an upper port (7.5-U), respectively.[4] A visible CCD camera with an interference filter for Hα emission measurement is installed in an outer port (3-O) for monitoring the plasma periphery and plasma-wall interactions near a lower port (2.5-L).[5] Three sets of ICRF antennae are set in 3.5, 4.5 and 7.5-U and -L ports for long pulse discharge experiments and ion heating.[6] Both sides of the antennae are protected by carbon limiters from heat load by the peripheral plasma. Figure 2(b) shows the divertor plate arrays in two helical sections viewed from an outer port. Langmuir probe arrays are embedded in five divertor plates (LP#1~#5). Dome-type electrodes (2 mm in diameter) are mounted along the edge of the divertor plates with 6 mm spacing. Thermocouples are located at the center of divertor plates (10 mm in depth) installed in every toroidal section where the plasma is horizontally and vertically elongated as shown in Figure 2(c) in order to measure the toroidal and poloidal distribution of the temperature of the divertor plates.

For estimating the distribution of the recycling neutral sources on the divertor plate arrays, magnetic field line tracing including a random walk process (as a particle diffusion) was carried out.[3] The magnetic field lines are traced from uniformly distributed points on the LCFS. Figure 3(a) shows the toroidal distribution of the number of strike points along the trace A and B (see Figure 2(a) and (b)) in the two different magnetic configurations (R_{ax}=3.60 m and 3.75 m). It indicates that while most of the magnetic field lines terminate on the inboard side of the torus for R_{ax}=3.60 m, they end locally at the upper and lower sides for R_{ax}=3.75 m. The close and open circles express the temperature rise of the divertor plates measured with thermocouples for the two magnetic configurations (R_{ax}=3.60 m and 3.75 m), respectively. The temperature

6

rise is normalized by the maximum value in each magnetic configuration. The toroidal distribution of the temperature rise qualitatively agrees with the calculations of the number of the strike points in both magnetic configurations.

The toroidal distribution of the power and the particle deposition on the divertor plates are calculated by a three-dimensional plasma fluid code coupled with a neutral particle transport simulation code (EMC3/EIRENE) which includes the effect of the particle and the energy transport in the peripheral plasma, which can explain the measured profile of the electron temperature in the ergodic layer, and that of neutral particles in the plasma periphery self-consistently.[7] Figure 3(b) illustrates the calculation of the toroidal distribution of the power (lines) and the particle (squares) deposition for the trace A in the two magnetic configurations. The calculated profiles qualitatively agree with those of the number of the strike points obtained by the magnetic field line tracing, indicating that the toroidal distribution of the power and particle deposition is estimated by the plasma transport along magnetic field lines. One of the reasons for the no significant difference between the calculation by the magnetic field line tracing and that of the simulation codes can be low neutral density in the plasma periphery due to low neutral pressure (<10 mPa) in the present divertor region (an open divertor configuration) in the LHD.

In order to investigate the relationship between the connection length of the magnetic field line (L_C) and the particle (ion flux) deposition on divertor plates, a test module with a Langmuir probe array was installed in an inner port. Figure 4(a) gives the experimental setup of a Langmuir probe array embedded in the test module installed in the inboard side of the torus. Figure 4(b) and (c) are the measurements of the ion saturation current profile (open circles) for the two magnetic configurations,

7

respectively.[4] It shows some peaks which position correspond to those with the long connection length (>several km) of the magnetic field lines (thin lines), and no contradiction between the measured profiles and the connection length ones. It supports that the estimation of the distribution of the power and particle deposition on the divertor plates by tracing the magnetic field lines from the LCFS is reasonable in the LHD plasmas.

The dependence of the distribution of the particle deposition on the radial position of the magnetic axis R_{ax} (shown in Figure 3) is also experimentally confirmed by observations with the H_α filtered visible CCD camera. Figure 5(a) and (b) give the Poincare plots of the ergodic layer at a vertically elongated plasma cross section and images of H_α emission in the two magnetic configurations, respectively. Gray broken squares represent the observation area of the CCD camera. The emission profiles in the two magnetic configurations are consistent with the magnetic field line distributions in lower divertor legs. It strongly suggests that the particle and power transport along the magnetic field lines are dominant in the LHD plasma periphery. These results also support the estimation of the particle and energy flux distributions on the divertor plate arrays by tracing magnetic field lines.

IV. NEUTRAL PARTICLE TRANSPORT ANALYSIS IN AN ICRF HEATED LONG PULSE DISCHARGE

Uncontrollable plasma density rise was observed in ICRF heated long pulse discharges (helium bulk and hydrogen minority heating) for R_{ax}=3.60 m.[8] The plasmas were terminated at around 150 s by radiation collapse. The single channel H_α emission

detector installed in the outer port (3-O) detected an observable Hα intensity rise in the latter half of the long pulse discharge (from ~90 s) as depicted in Figure 6. The toroidal and poloidal distribution of divertor plate temperature show the maximum temperature rise at 3-I port (~400 degrees centigrade). The CCD camera observed a hot spot on a vertically installed divertor plate near a lower port (2.5-L).[5] The hot spot was observed only during ICRF heating by antennae installed in 3.5-L and 3.5-U ports. A bright thin line above a divertor leg near the lower port was also observed only during the ICRF heating.

In order to investigate the effect of accelerated protons by ICRF waves on the formation of the hot spot, the trajectories of the protons are calculated by a particle orbit analysis code in which the initial points of the protons locate along a minority ion cyclotron resonance layer just in front of the antennae in 3.5-L and -U ports.[9] The calculation shows that the toroidal and poloidal distribution of the temperature rise of divertor plates is explained by the distribution of the strike points of the accelerated protons. It also indicates that the strike points of the accelerated protons concentrate on the position of the hot spot (2.5-L port). The bright thin line is also explained by the trajectory of the accelerated protons from the resonance layer in front of the lower antenna (3.5-L port).

For identifying the primary source of the neutral particle fueling which induced the uncontrollable plasma density rise in the long pulse discharge, a three-dimensional neutral particle transport simulation code (DEGAS ver.63) was applied.[10] In the simulation code, many test particles representing neutral hydrogen atoms and molecules are launched into a three-dimensional grid model, and the trajectories of the test particles are determined by the Monte Carlo method including the reactions of atomic

and molecular processes in plasmas. The toroidal distribution of the H_α intensity is calculated by integrating the emission along the line of sight of the detectors. Pure helium plasma is assumed in this simulation, the spatial profile of the plasma parameters inside the ergodic layer and on the divertor legs is based on the measurements, and the distribution of neutral particle source (hydrogen atoms and molecules) released from the divertor plates was defined by the distribution of the strike points calculated by the trajectory analysis of the accelerated protons.

Figure 7(a) gives the toroidal profile of the measured H_α intensity rise (the ratio of the intensity at the plasma termination (150 s) to that before the intensity rise (90 s)), showing two peaks at 3-O and 10-O ports. Figure 7(b) is the toroidal profile of the calculated H_α intensity due to gas fueling induced by the accelerated protons. The calculation shows two peaks around 4-O and 9-O ports, which qualitatively agrees with the measured toroidal profile of the H_α intensity rise. Open circles represent the calculation of the toroidal profile of the H_α intensity in the case where the neutral particles are locally released from the vertically installed divertor plate (2.5-L port) on which the hot spot was observed by the CCD camera. The calculation shows locally peak profile of the intensity around 3-O port, which cannot explain the measured two peaks of the H_α intensity rise. Open triangles indicate the calculated toroidal profile of the H_α intensity due to neutral particles locally released from the carbon limiter for protecting the ICRF antennae installed in 2.5-U and 2.5-L ports. While the calculation shows the peaked profile around 3-O port, the second peak in around 10-O port cannot be explained by the neutral particles released from the carbon limiter.[11]

The three-dimensional neutral particle transport simulation code reveals that local

gas fueling from the position of the hot spot and of the carbon limiter alone cannot explain the measurement, indicating that toroidally distributed neutral particle sources are necessary for explaining the whole measured toroidal H_α intensity profile in the long pulse discharge. Neutral particles released from toroidally distributed divertor plates heated by the accelerated protons are indispensable for explaining the uncontrollable neutral particle fueling (the H_α intensity rise) in the ICRF heated long pulse discharge. The dependence of particle desorption from the divertor plates on the temperature was investigated by an electron beam irradiation facility, indicating significant neutral particle desorption for around 300 degrees centigrade.[12] It can explain the measured H_α intensity rise in the latter half of the long pulse discharge as shown in Figure 6. It strongly suggest that suppression of neutral particle fueling from the divertor plates heated by the accelerated protons is effective for extending of the plasma duration time in ICRF heated long pulse discharges.

V. MAGNETIC AXIS SWING OPERATION FOR HEAT LOAD REDUCTION ON DIVERTOR PLATES

The neutral particle transport analysis in the ICRH heated long pulse discharge strongly suggests that mitigation of the heat load on the divertor plates is effective for suppression of neutral particle fueling from divertor plates. The toroidal and poloidal distribution of the strike points are significantly different in the two magnetic configurations (R_{ax}=3.60 m and 3.75 m). The heat load is mainly deposited in the inboard side and the lower/upper side of the torus in these two magnetic configurations,

respectively, as shown in Figure 3(b). For this reason, it is effective for reduction of the heat load on the divertor plates to swing the radial position of the magnetic axis R_{ax} in the range between 3.60 m and 3.75 m.

The magnetic axis swing operation was tried to optimize the range of the swing in ICRF heated long pulse discharges. Figure 8(a) shows the time evolutions of the temperature rise of divertor plates installed in an inboard side (#1) and a lower/inner side (#6) (See Figure 2(c)) measured during a magnetic axis swing operation (3.62 m<R_{ax}<3.65 m). The temperature of the divertor plates monotonically increases, indicating no effective suppression of the temperature rise. Figure 8(b) shows the time evolution of the temperature during a magnetic axis swing operation (3.65 m<R_{ax}<3.69 m). The temperature rise of the divertor plates was actively controlled and heat load was almost uniformly dispersed to the two divertor plates. The dispersion of the particle deposition on the two divertor plates by the magnetic axis swing operation was also observed with the Langmuir probe arrays.[13]

The magnetic axis swing operation (3.65 m<R_{ax}<3.69 m) proved to be effective for dispersing the heat and particle deposition on the divertor plates. It successfully contributed to further extension of the plasma duration time in ICRF heated long pulse discharges (more than 500 s) by suppressing the uncontrollable neutral particle fueling, which can be supported by installation of new divertor plates with a good heat removal efficiency.[14]

VI. ANALYSIS OF NEUTRAL PARTICLE TRANSPORT IN THE LHD PLASMA PERIPHERY

Control of the neutral particles released from the divertor plates is an important issue not only for long pulse discharges but also for achieving SDC plasmas. Investigation of neutral particle transport in various magnetic configurations is essential for understanding the divertor function and for optimization of a future closed helical divertor configuration.

Neutral particles in the plasma periphery have been measured with multi-channel H_α emission detector arrays with polarization separation optics for identifying the location and the intensity of the emission on the line of sight of the detectors in various magnetic configurations.[15] Figure 9(a) and (b) show the spatial profile of the H_α emission on the poloidal cross section of the vertical array of the H_α emission detectors in the two different magnetic configurations (R_{ax}=3.60 m and 3.75 m), respectively. The measurements indicate that the H_α emission locates in the edge of the ergodic layer or on the divertor legs. It also shows that the prominent H_α emission area changes from the inboard side to the outboard side with the increase in the radial position of the magnetic axis R_{ax}.

For detailed understanding of neutral particle transport in various magnetic configurations, a three-dimensional neutral particle transport code (EIRENE) was applied.[16] The toroidal and poloidal distribution of gas fueling from the divertor plates was determined by the calculation of magnetic field line tracing from the LCFS including the particle diffusion effect. Plasma parameter profiles in the code are fixed to be experimental results measured with plasma diagnostic systems (a multi-chord far-infrared interferometer, YAG laser Thomson scattering, charge exchange recombination spectroscopy and a reciprocating-type fast scanning Langmuir probe and

so on). Figure 10(a) and (b) indicate the calculated profiles of the H_α emission on the detector's surface of the vertical array for R_{ax}=3.60 m and 3.75 m, respectively. It reproduces change of the position of prominent H_α emission area from the inboard side to the outboard side with the increase in the radial position of the magnetic axis R_{ax}.[17]

Line integrated H_α intensity profiles along the line of sight of the detectors can also be calculated by the simulation code. Figure 11(a) shows the intensity profile measured with the vertical and the horizontal detector arrays for R_{ax}=3.60 m. The line of sight of the two H_α emission detector arrays is also indicated in the figures. Figure 11(b) gives the intensity profiles calculated by integrating the H_α emission along the line of sight of the vertical and the horizontal arrays. The calculations are qualitatively in agreement with the measurements, indicating that the neutral particle transport simulation is effective for the analysis of the divertor function and of neutral particle transport in the peripheral plasma because of reasonable agreement with the measurements in the different two magnetic configurations.

VII. DESIGN OF A CLOSED HELICAL DIVERTOR CONFIGURATION FOR EFFICIENT PARTICLE CONTROL

For efficient particle control in the LHD plasma periphery, installation of a closed helical divertor (CHD) is planned in the near future. It can be effective for controlling the plasma density and for achieving divertor detachment which has not stably sustained in LHD plasmas yet. On the basis of the neutral particle transport analysis in various magnetic configurations, the inward shift magnetic configuration (R_{ax}=3.60 m) is the

best choice for the closed divertor configuration because the neutral particle density is relatively high in the inboard side, which is advantageous for efficient particle pumping from the inboard side, and the best plasma confinement time has been achieved in this magnetic configuration.[18] Measurements with a fast ion gauge installed in the inboard side indicate that the typical neutral particle pressure is less than 10 mPa for R_{ax}=3.60 m.[19] A simple particle balance analysis during fueling pellet injection predicts that the neutral particle pressure is not enough for achieving efficient particle control. Thus, enhancement of the neutral pressure by more than one-order of magnitude is necessary.

The CHD configuration has been optimized for achieving enhancement of the neutral particle pressure in the inboard side.[20] Figure 12 shows a schematic view of the plan of the CHD configuration which practically utilizes the three-dimensional structure of the magnetic field lines in the LHD plasma periphery for R_{ax}=3.60 m. The components of the CHD are installed along the space between the two helical coils only in the inboard side because the magnetic field line tracing shows that more than 80% of the strike points locate there. The CHD consists of the following three components:

1. V-shaped dome which can efficiently confine the neutral particles in the inboard side, and hinder penetration of neutral particles into the ergodic layer and ionization near X-points in the inboard side. The plasma produced by the ionization inside the ergodic layer moves along the long magnetic field lines, which increases the peripheral plasma density. The neutral particles released from the divertor plates are accumulated behind the dome, and pumped out with vacuum pumps installed along the space between the two helical coil cans.

2. Slanted divertor plates to the inboard side such that neutral particles/impurities released from the divertor plates go toward the backside of the dome. The arrangement

of the divertor plates functions as a baffle for preventing the outflow of the neutral particles from the divertor region into the main plasma. Most of the neutral particles in this configuration are ionized by plasmas on the divertor legs due to the small conductance between the divertor plates and the dome.

3. Target plates vertically installed at both toroidal ends of the CHD components. The plates hinder toroidal outflow of neutral particles along the space between the two helical coil cans toward upper/lower ports, and change the distribution of strike points from the upper/lower side to the inboard side because the target plates intersect the magnetic field lines on the divertor legs. The directions of magnetic field lines on two adjacent divertor legs across X-points are opposite, that is while magnetic field lines on a lower divertor leg are directly connect to the inboard side, magnetic field lines on another divertor leg connect to the outboard side. The target plates are placed so as to intersect only the latter divertor leg for enhancing the neutral particle density in the inboard side.

Figure 13 is the Poincare plots (including the diffusion effect) of the magnetic field lines in the plasma periphery for R_{ax}=3.60 m in a poloidal cross section where the plasma is horizontally elongated in the case with the CHD components. The CHD has the following three main advantages over other closed divertor concepts:

1. The strongly ergodized divertor legs in the inboard side for R_{ax}=3.60 m contribute extending the plasma wetted area on the slanted divertor plates which is roughly estimated to about 5 m^2 by the magnetic field line tracing. Thanks to the large plasma wetted area, it is effective for mitigation of the heat load on the divertor plates. The plasma on the ergodized divertor legs prevents the outflow of the neutral particles from the divertor region to the main plasma due to the effect of the ionization of neutral

particles on the divertor legs.

2. The curved divertor legs toward the inboard side of the torus are favorable for efficient particle control/pumping from the inboard side. This is because most of neutral particles and impurities released from the slanted divertor plates go toward to the entrance of the vacuum pumps.

3. Most of the strike points (~80%) are directly connected to the divertor and the target plates for R_{ax}=3.60 m. It is favorable for neutral particle control because the neutral particles are efficiently pumped out from the inboard side with no interference with plasma heating and diagnostic systems which have to be installed in the outboard side.

In addition to the above three advantages, the ergodic layer functions as a shield against impurity penetration, which has been experimentally confirmed by comparing the measurements of carbon emission profiles and the calculations by the three-dimensional plasma fluid code (EMC3-EIRENE).[21] The analysis indicates that friction force and remnant magnetic islands have significant effect on impurity retention in the ergodic layer. It is possible that the long magnetic field lines in the ergodic layer are effective for cooling down the plasma temperature due to radiation by impurities in the plasma periphery.[22]

The spatial profile of the neutral particle density was calculated in the CHD configuration by using the neutral particle transport simulation code coupled with a one-dimensional plasma fluid analysis on the divertor legs in which volume source effects by recombination processes is included. In this calculation, the spatial profile of plasma parameters inside the ergodic layer are fixed to the calculation by the plasma fluid code (EMC3-EIRENE) in the case of P_{input}=8 MW, n_e^{LCFS}~4×10^{19} m^{-3},

$\Gamma_{\text{total}}=3.6\times10^4$ A, where P_{input} is an input power from the LCFS into the ergodic layer, $n_{\text{e}}^{\text{LCFS}}$ is a plasma density at the LCFS, and Γ_{total} is a total plasma outflow current transported from the ergodic layer. A recycling coefficient on the divertor plates R_{div} is assumed to 0.65, which leads to a reasonable neutral particle pressure being consistent with the measurements in the inboard side for the present open divertor. The particle reflection coefficient on the surface of the vacuum pumping system is set to 0.9 in this calculation. The spatial profile of the neutral particle density and plasma parameters on the divertor legs is determined by an iteration process between the plasma parameter profiles on the divertor legs and the neutral particle density profiles. Figure 14 gives the calculation of the three poloidal cross sections of the pressure profile of neutral hydrogen molecules in the CHD configuration for $R_{\text{ax}}=3.60$ m. The molecular hydrogen density behind the dome in the inboard side is high (more than ~0.3 Pa), which is enough for achieving efficient particle pumping. Most (~80%) of neutral particles in the divertor region are ionized on the divertor legs. It indicates that plasmas produced by the ionization of neutral particles released from the divertor plates are almost recycled in the divertor region. A CHD configuration has been successfully designed for the LHD, which can contribute to further extension of the plasma duration time in ICRF heated long pulse discharges, sustainment of SDC plasmas with reduced peripheral plasma density, and divertor detachment due to high density of neutral hydrogen molecules in the divertor region.

VIII.　SUMMARY

The functions of the helical divertor have been investigated from viewpoints of

measurements and numerical calculations by magnetic field line tracing. It indicates that the toroidal and poloidal distribution of the power and particle deposition on the divertor plates is estimated by tracing magnetic field lines in the plasma periphery with a particle diffusion effect. It is numerically supported by the calculation of a three-dimensional plasma fluid code (EMC3/EIRENE) which includes the effect of recycling neutral particles and energy transport self-consistently. A Langmuir probe array embedded in the test module installed in the inboard side shows the some peaked profiles of the ion saturation current. The positions of the peaks correspond to those with the long connection length of the magnetic field lines (> several km). It supports that the distribution of the power and particle deposition on the divertor plates are estimated by tracing the magnetic field lines. The neutral particle transport simulation indicates that control of the neutral particle fueling from the divertor plate is a critical issue for extending the plasma duration time in ICRF heated long pulse discharges. Measurements of the spatial profile of H_α emission and the neutral particle transport analyses in various magnetic configurations clearly show that an inward shift magnetic configuration (R_{ax}=3.60 m) is the favorable for the closed helical divertor (CHD) configuration. By practically using the intrinsic three-dimensional magnetic field line structure in the LHD plasma periphery, efficient particle control can be achieved in the optimized CHD configuration. The CHD is also effective for sustaining ICRF heated long pulse discharges by actively pumping neutral particles released from divertor plates heated by accelerated protons by ICRF waves.

FIGURE CAPTIONS

Fig. 1. Poincare plots of the magnetic field lines in the main plasma confinement region, the ergodic layer and the divertor legs in a horizontally elongated plasma cross section for two different magnetic configurations (R_{ax}=3.60 m and 3.75 m).

Fig. 2. (a) An equatorial cross section of the LHD vacuum vessel. (b) Schematic view of the divertor plate arrays (labeled A and B) for two toroidal pitch angles (72°). (c) Positions of the thermocouples embedded in the divertor plates in horizontally and vertically elongated plasma cross sections.

Fig. 3. (a) Toroidal distribution of the number of the strike points (lines) and normalized temperature rise of the divertor plates (circles). Thin (bold) lines and closed (open) circles correspond to ones for R_{ax}=3.60 m and 3.75 m, respectively. Traces A and B mean the divertor arrays labeled A and B shown in Figure 2(a) and (b), respectively. (b) Toroidal distribution of the particle (squares) and the power (lines) depositions for the trace A calculated by the EMC3/EIRENE code in the two magnetic configurations (R_{ax}=3.60 m and 3.75 m).

Fig. 4. (a) Experimental setup of a Langmuir probe array embedded in a test module installed in the inboard side of the torus. Profiles of the ion saturation current (open circles) measured in the magnetic configurations R_{ax}=3.60 m (b) and 3.75 m (c). Thin black lines mean the profiles of the connection length of magnetic field lines on the test module of the probe array.

Fig. 5. (a) Poincare plots of the magnetic field lines in the ergodic layer and the divertor legs in magnetic configurations R_{ax}=3.60 m and 3.75 m in a vertically elongated plasma cross section. (b) Images of H_α emission in the plasma periphery near a lower port (2.5-L) observed with the CCD camera in the two magnetic configurations (R_{ax}=3.60 m and 3.75 m).

Fig. 6. Time traces of the rate of gas fueling, plasma density, H_α and HeI intensity and the temperature of a divertor plate installed near 3-I port measured in an ICRF heated long pulse discharge for R_{ax}=3.60 m.

Fig. 7. (a) The toroidal profile of the ratio of the H_α intensity rise measured in an ICRH heated long pulse discharge. (b) The calculations of the toroidal profile of the H_α intensity due to the gas fueling induced by accelerated protons by ICRF waves, the hot spot (circles), and the carbon limiter for ICRF antennae (triangles). These calculations are normalized to the H_α intensity in 3-O port.

Fig. 8. Temperature rise of divertor plates installed in the inboard side (#1) and lower side (#6) during magnetic axis swing operations in the range between R_{ax}=3.62 m and 3.65 m (a) and between R_{ax}=3.65 m and 3.69 m (b). The time trends of the radial position of the magnetic axis during the operations are also indicated.

Fig. 9. The measurements of the H_α emission spatial profile obtained by the analysis of the polarization resolved H_α spectra for R_{ax}=3.60 m (a) and 3.75 m (b). The size of the

open circles expresses the intensity of the emission at the center of the circles on the line of sight of the detectors.

Fig. 10. The spatial profile of H_α emission calculated by the neutral particle transport simulation code on the detector's surface of the vertical array for R_{ax}=3.60 m (a) and 3.75 m (b).

Fig. 11. Intensity profiles of H_α emission measured with the vertical (1-O) and horizontal detector array (7.5-U) for R_{ax}=3.60 m (a), and the calculations obtained by the neutral particle transport simulation code (b).

Fig. 12. A schematic view of the plan of the closed helical divertor configuration installed in the inboard side of the torus for one toroidal pitch angle (36°).

Fig. 13. Poincare plots of the magnetic field lines in the plasma periphery for R_{ax}=3.60 m with a poloidal cross section of the closed helical divertor components in a horizontally elongated plasma cross section.

Fig. 14. Three poloidal cross sections of the pressure profile of neutral hydrogen molecules in the closed helical divertor configuration for R_{ax}=3.60 m. The area with high density of neutral hydrogen molecules (more than ~0.3 Pa) is formed behind the dome and near the target plates in the inboard side of the torus.

R_{ax}=3.60m

Inboard

Magnetic Axis

Outboard

Divertor Leg

Divertor Plates

Vacuum Vessel

R_{ax}=3.75m

Ergodic Layer

Helical Coil
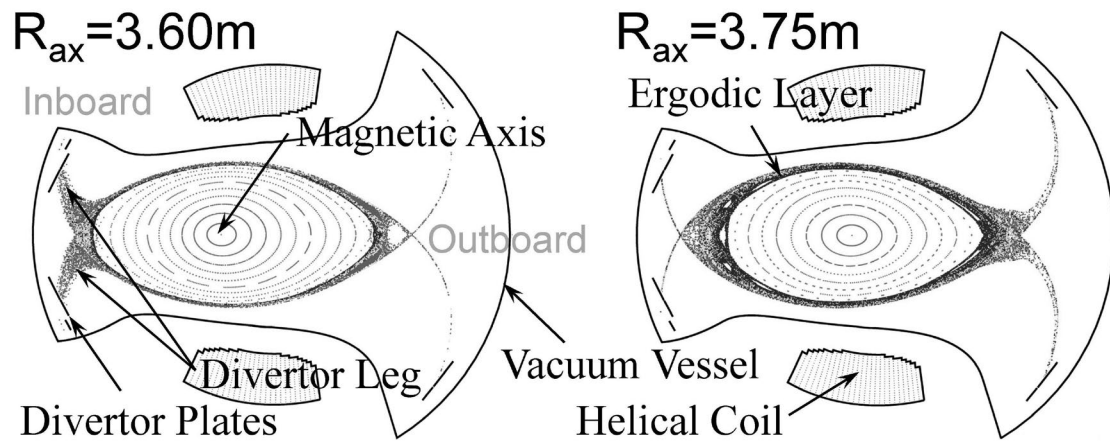
Fig. 1. M. SHOJI et al., INVESTIGATION OF THE HELICAL DIVERTOR FUNCTION AND THE FUTURE PLAN OF A CLOSED DIVERTOR FOR EFFICIENT PARTICLE CONTROL IN THE LHD PLASMA PERIPHERY
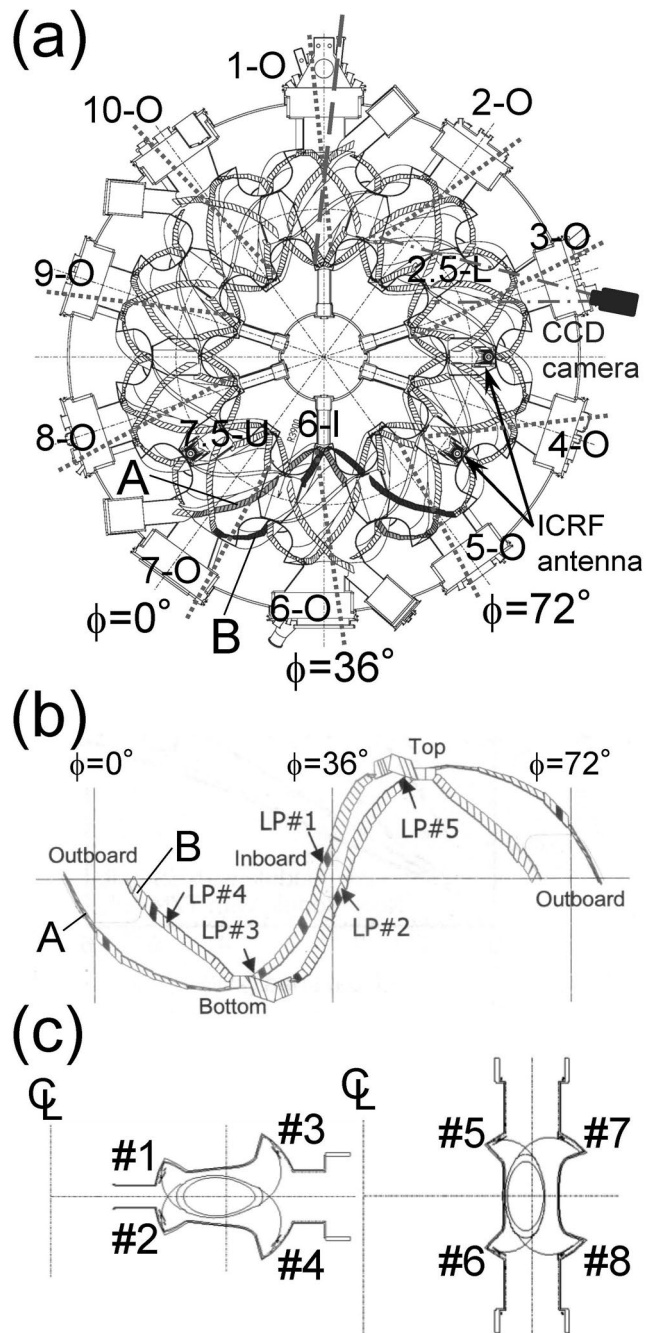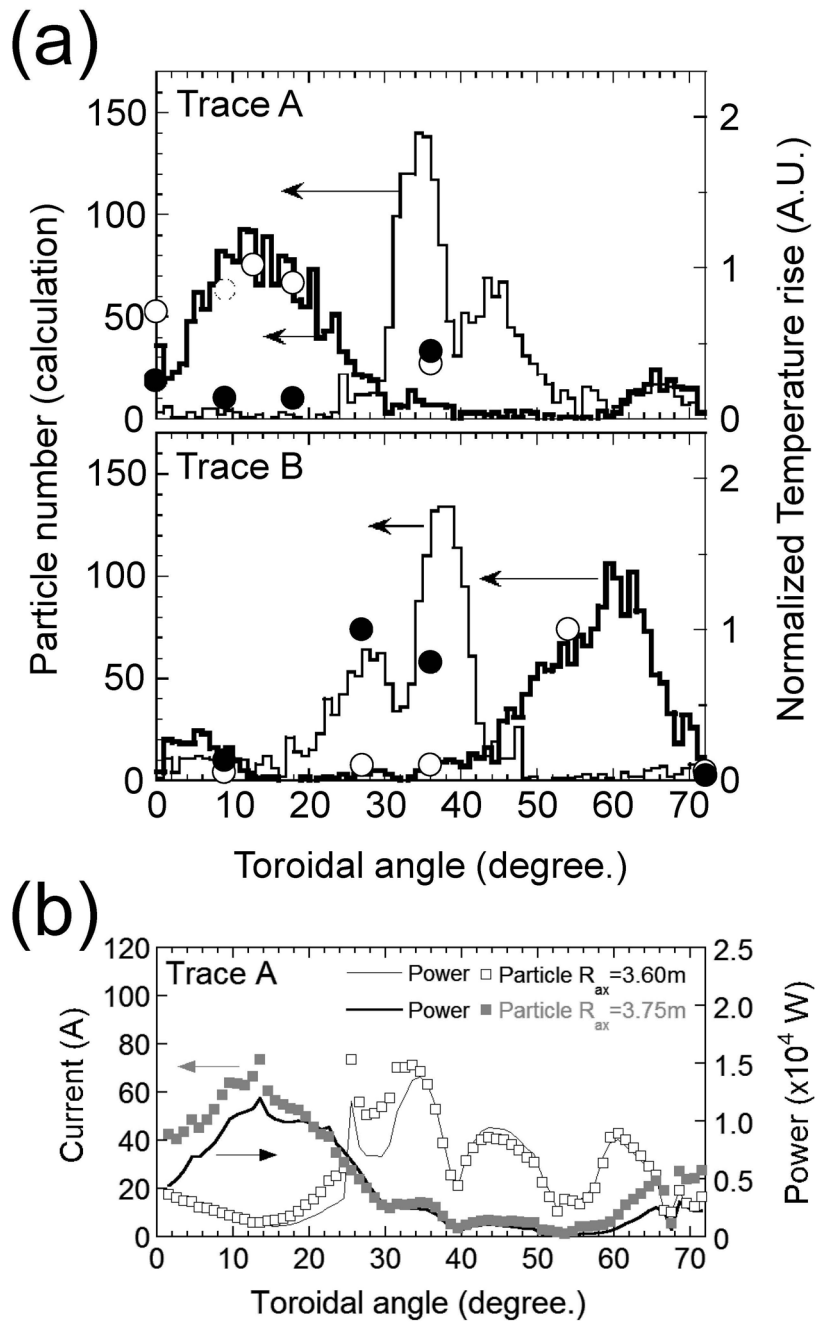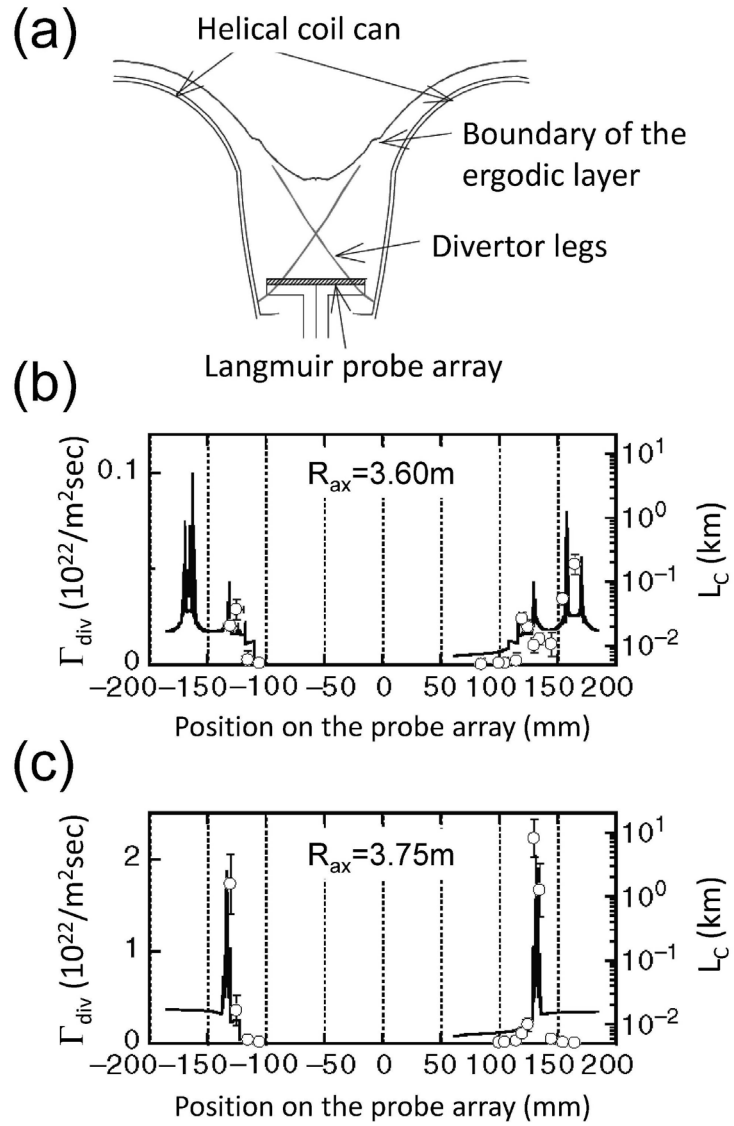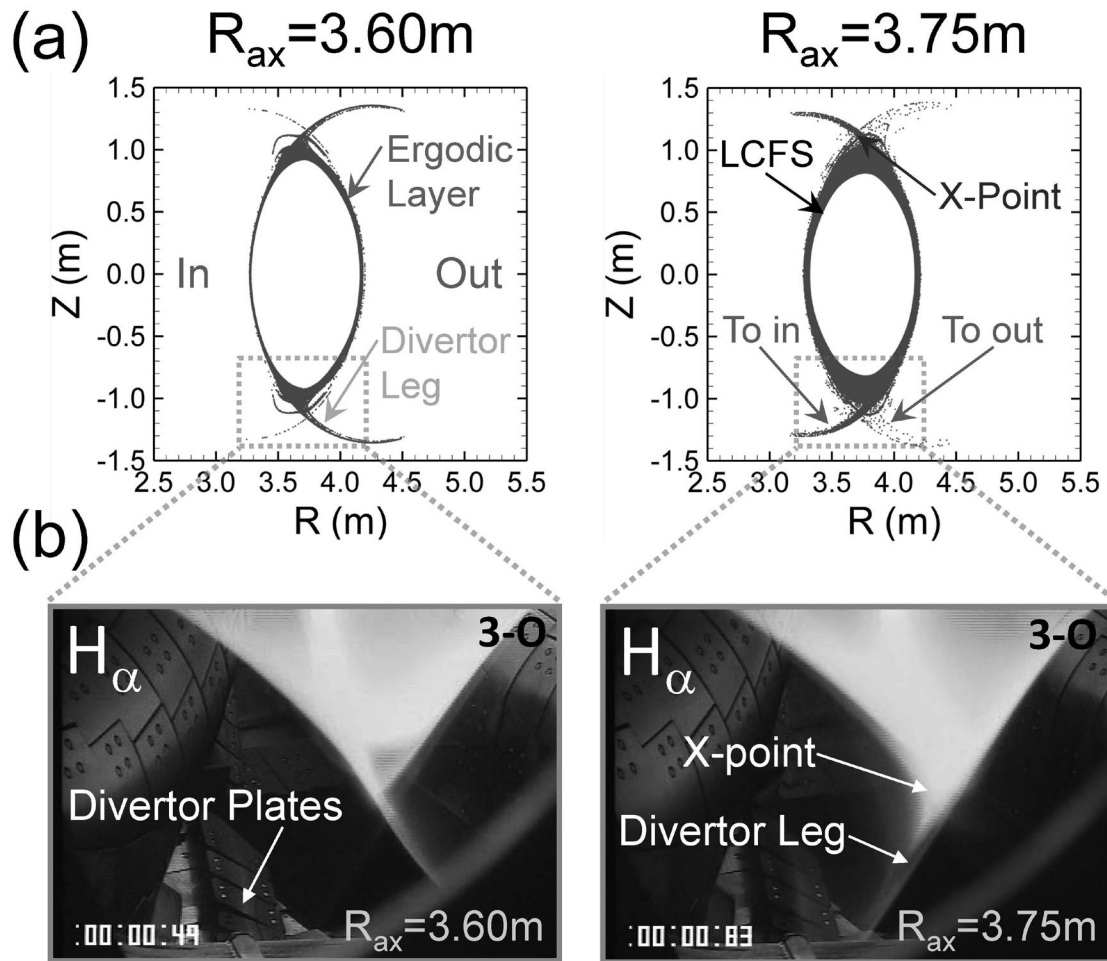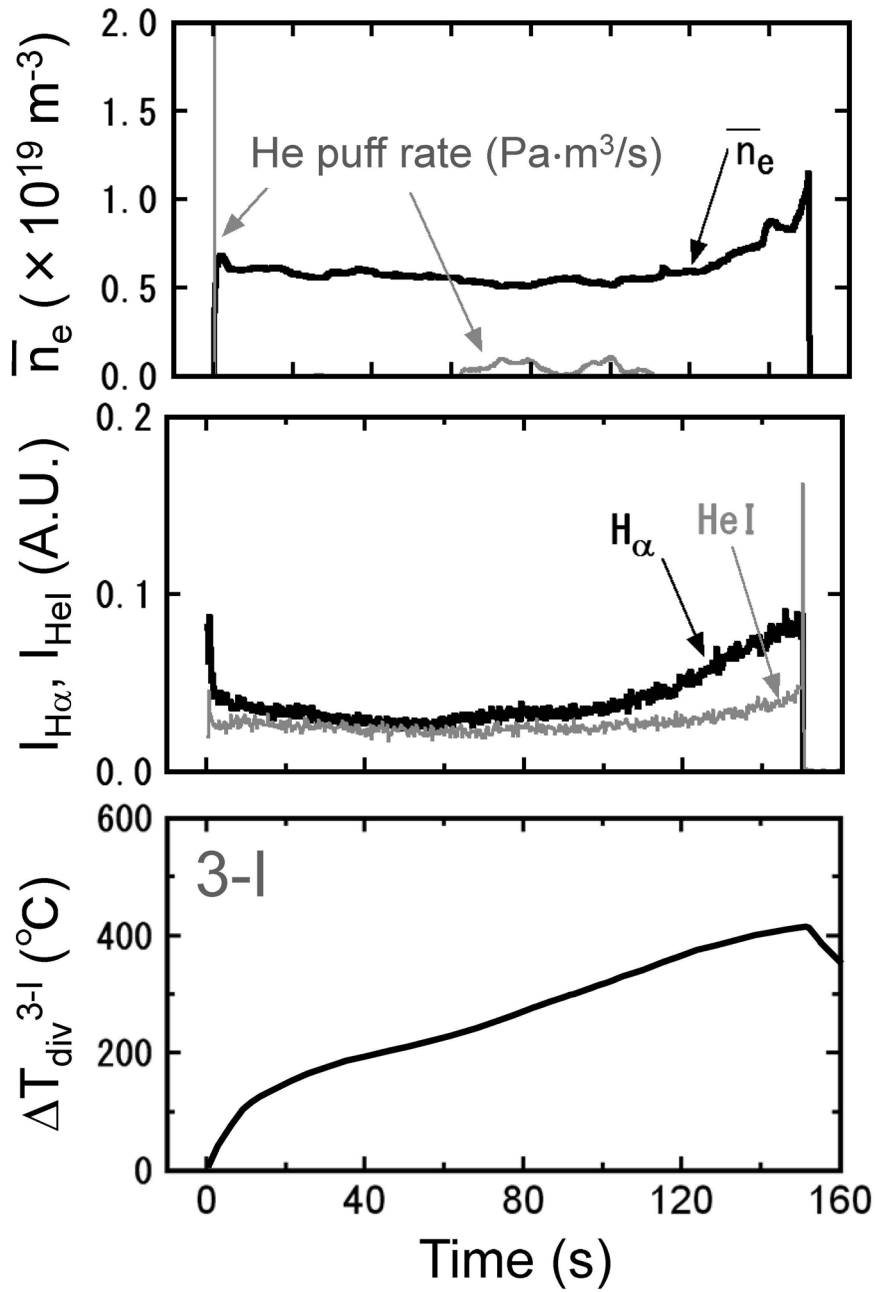
Fig. 2. M. SHOJI et al., INVESTIGATION OF THE HELICAL DIVERTOR FUNCTION AND THE FUTURE PLAN OF A CLOSED DIVERTOR FOR EFFICIENT PARTICLE CONTROL IN THE LHD PLASMA PERIPHERY
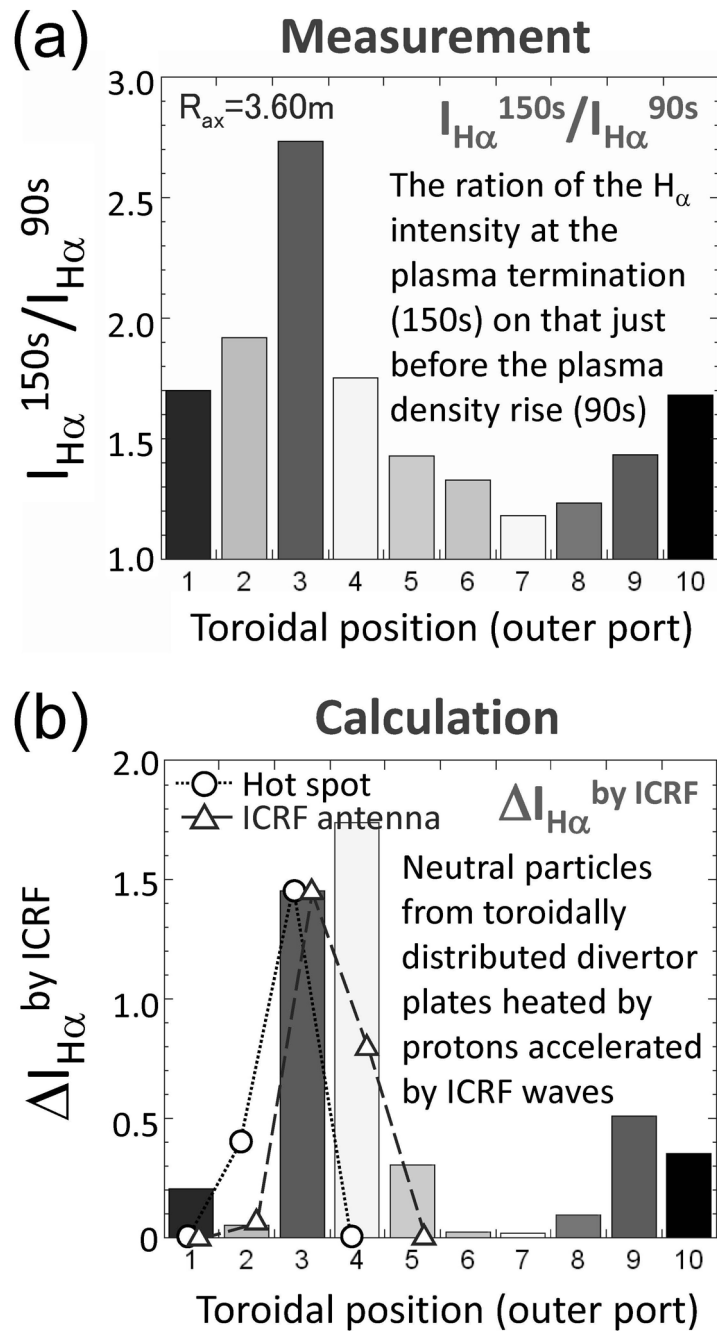
Fig. 3. M. SHOJI et al., INVESTIGATION OF THE HELICAL DIVERTOR FUNCTION AND THE FUTURE PLAN OF A CLOSED DIVERTOR FOR EFFICIENT PARTICLE CONTROL IN THE LHD PLASMA PERIPHERY

Fig. 4. M. SHOJI et al., INVESTIGATION OF THE HELICAL DIVERTOR FUNCTION AND THE FUTURE PLAN OF A CLOSED DIVERTOR FOR EFFICIENT PARTICLE CONTROL IN THE LHD PLASMA PERIPHERY
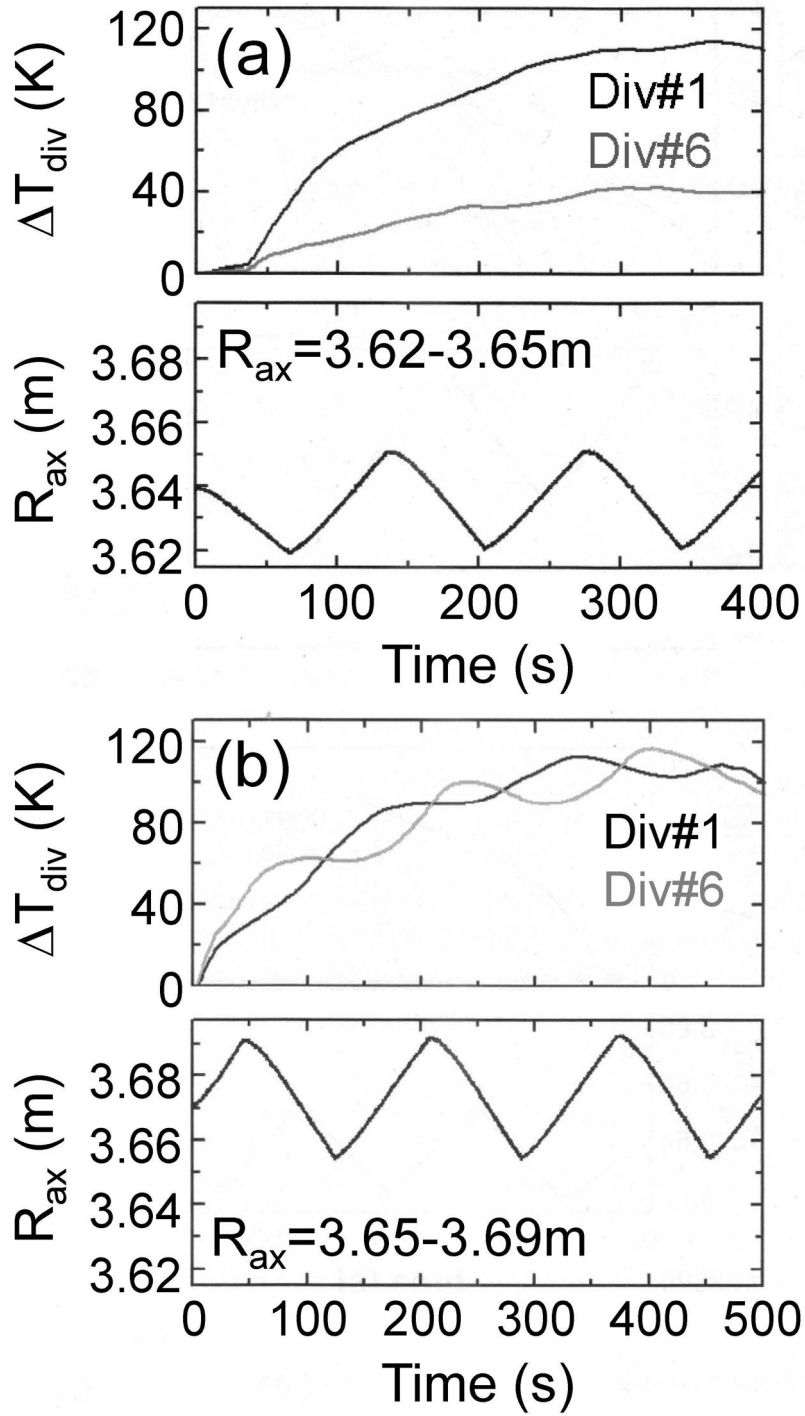
Fig. 5. M. SHOJI et al., INVESTIGATION OF THE HELICAL DIVERTOR FUNCTION AND THE FUTURE PLAN OF A CLOSED DIVERTOR FOR EFFICIENT PARTICLE CONTROL IN THE LHD PLASMA PERIPHERY

Fig. 6. M. SHOJI et al., INVESTIGATION OF THE HELICAL DIVERTOR FUNCTION AND THE FUTURE PLAN OF A CLOSED DIVERTOR FOR EFFICIENT PARTICLE CONTROL IN THE LHD PLASMA PERIPHERY
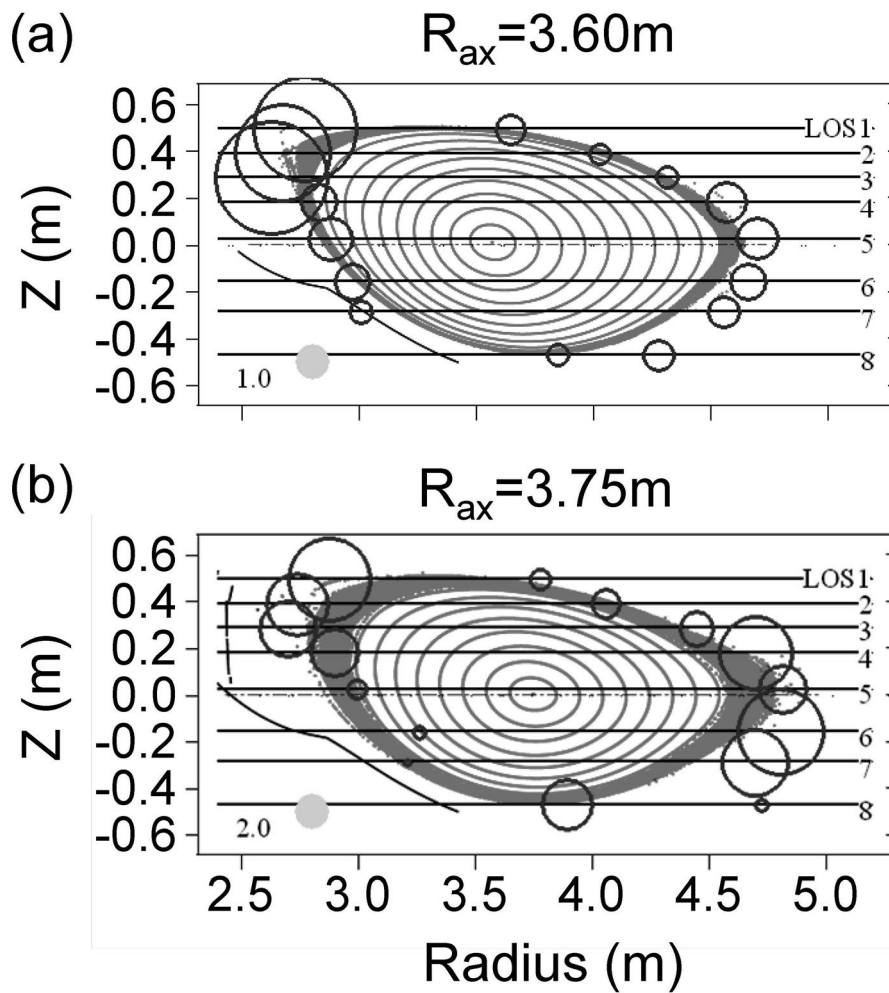
Fig. 7. M. SHOJI et al., INVESTIGATION OF THE HELICAL DIVERTOR FUNCTION AND THE FUTURE PLAN OF A CLOSED DIVERTOR FOR EFFICIENT PARTICLE CONTROL IN THE LHD PLASMA PERIPHERY

Fig. 8. M. SHOJI et al., INVESTIGATION OF THE HELICAL DIVERTOR FUNCTION AND THE FUTURE PLAN OF A CLOSED DIVERTOR FOR EFFICIENT PARTICLE CONTROL IN THE LHD PLASMA PERIPHERY
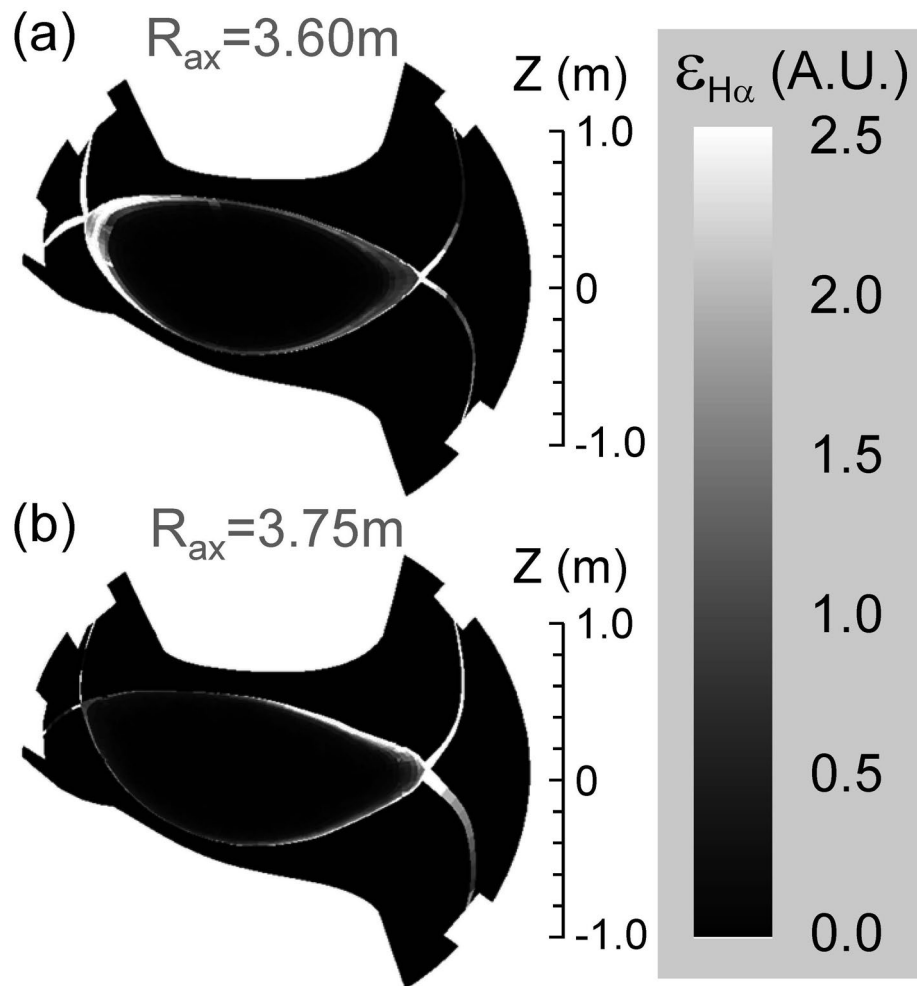
Fig. 9. M. SHOJI et al., INVESTIGATION OF THE HELICAL DIVERTOR FUNCTION AND THE FUTURE PLAN OF A CLOSED DIVERTOR FOR EFFICIENT PARTICLE CONTROL IN THE LHD PLASMA PERIPHERY

(a) R_{ax}=3.60m

(b) R_{ax}=3.75m

Z (m)

$\varepsilon_{H\alpha}$ (A.U.)

Fig. 10. M. SHOJI et al., INVESTIGATION OF THE HELICAL DIVERTOR FUNCTION AND THE FUTURE PLAN OF A CLOSED DIVERTOR FOR EFFICIENT PARTICLE CONTROL IN THE LHD PLASMA PERIPHERY
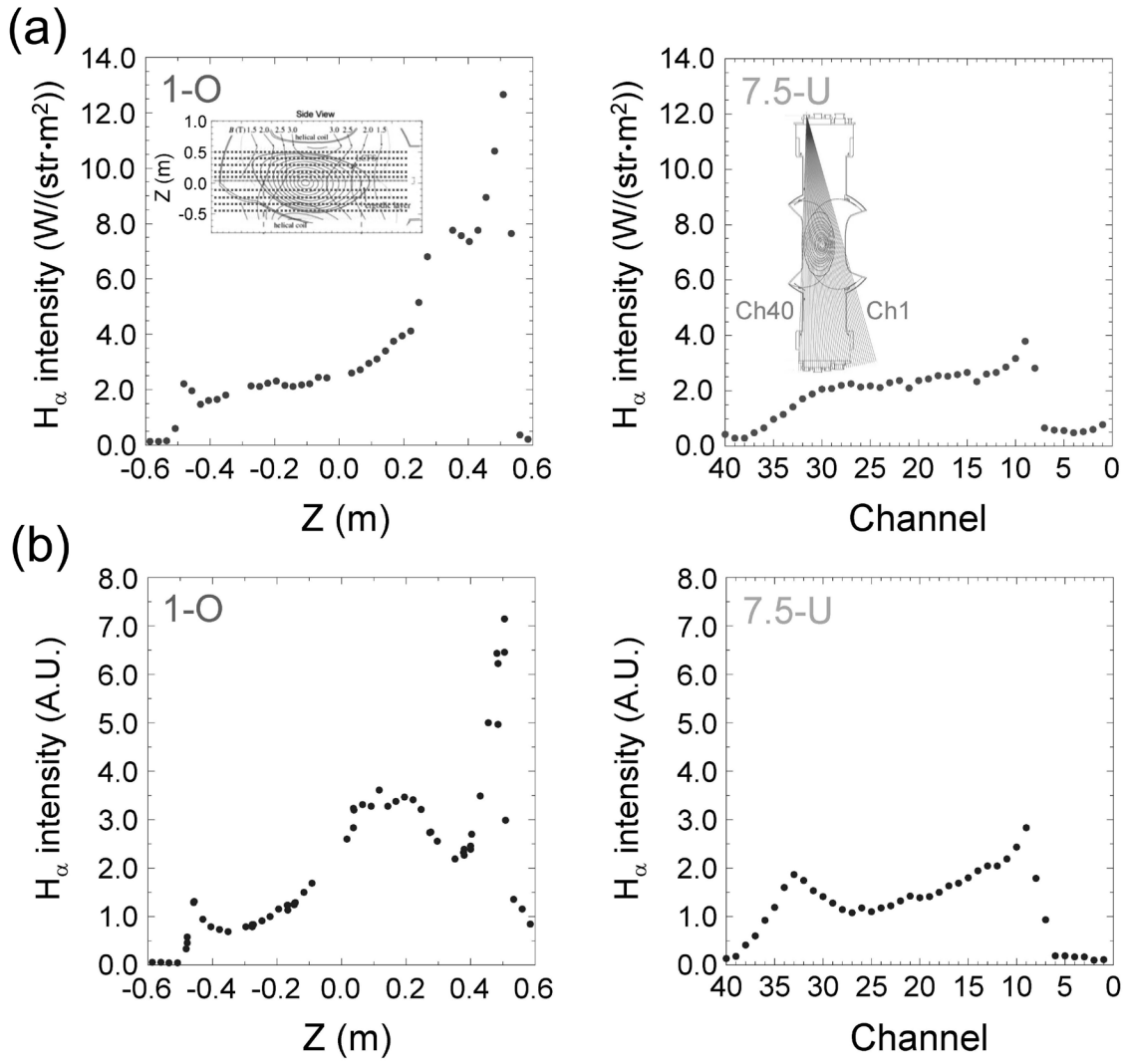
Fig. 11. M. SHOJI et al., INVESTIGATION OF THE HELICAL DIVERTOR FUNCTION AND THE FUTURE PLAN OF A CLOSED DIVERTOR FOR EFFICIENT PARTICLE CONTROL IN THE LHD PLASMA PERIPHERY
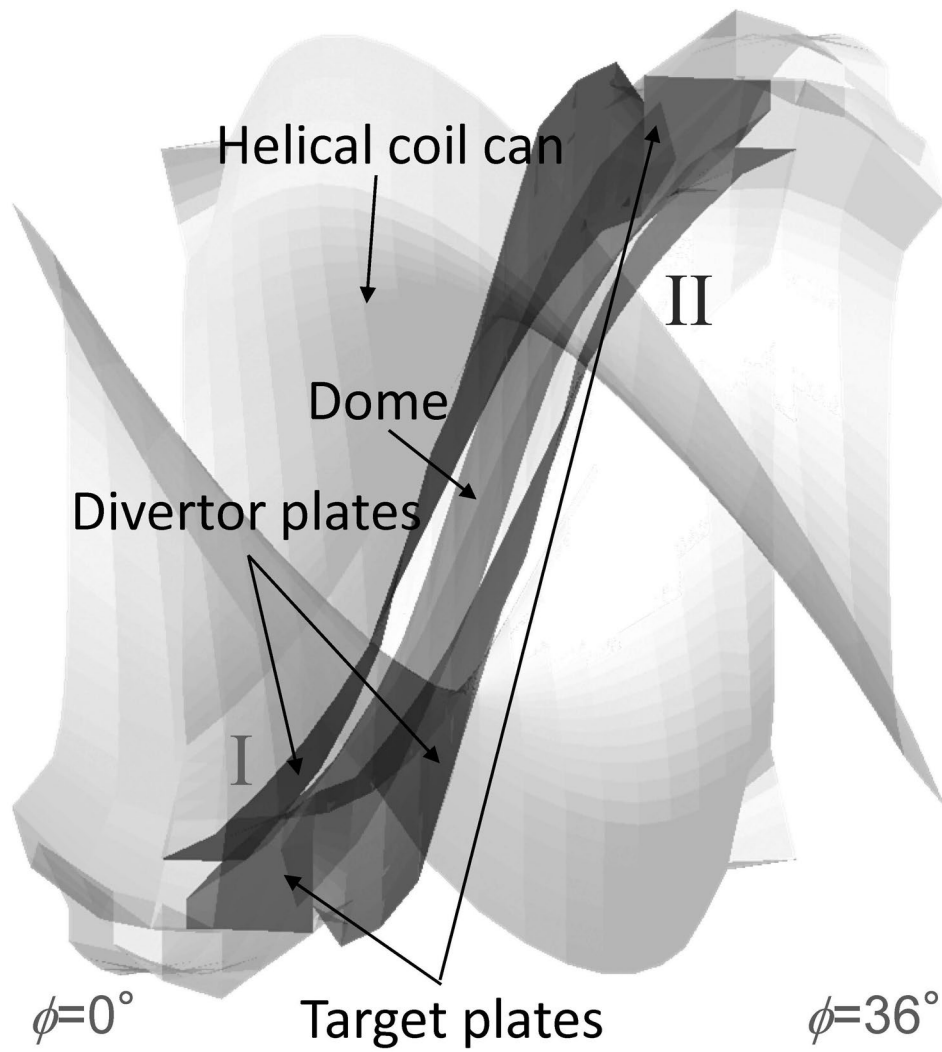
Helical coil can

Dome

Divertor plates

II

I

ϕ=0°

Target plates

ϕ=36°

Fig. 12. M. SHOJI et al., INVESTIGATION OF THE HELICAL DIVERTOR
FUNCTION AND THE FUTURE PLAN OF A CLOSED DIVERTOR FOR
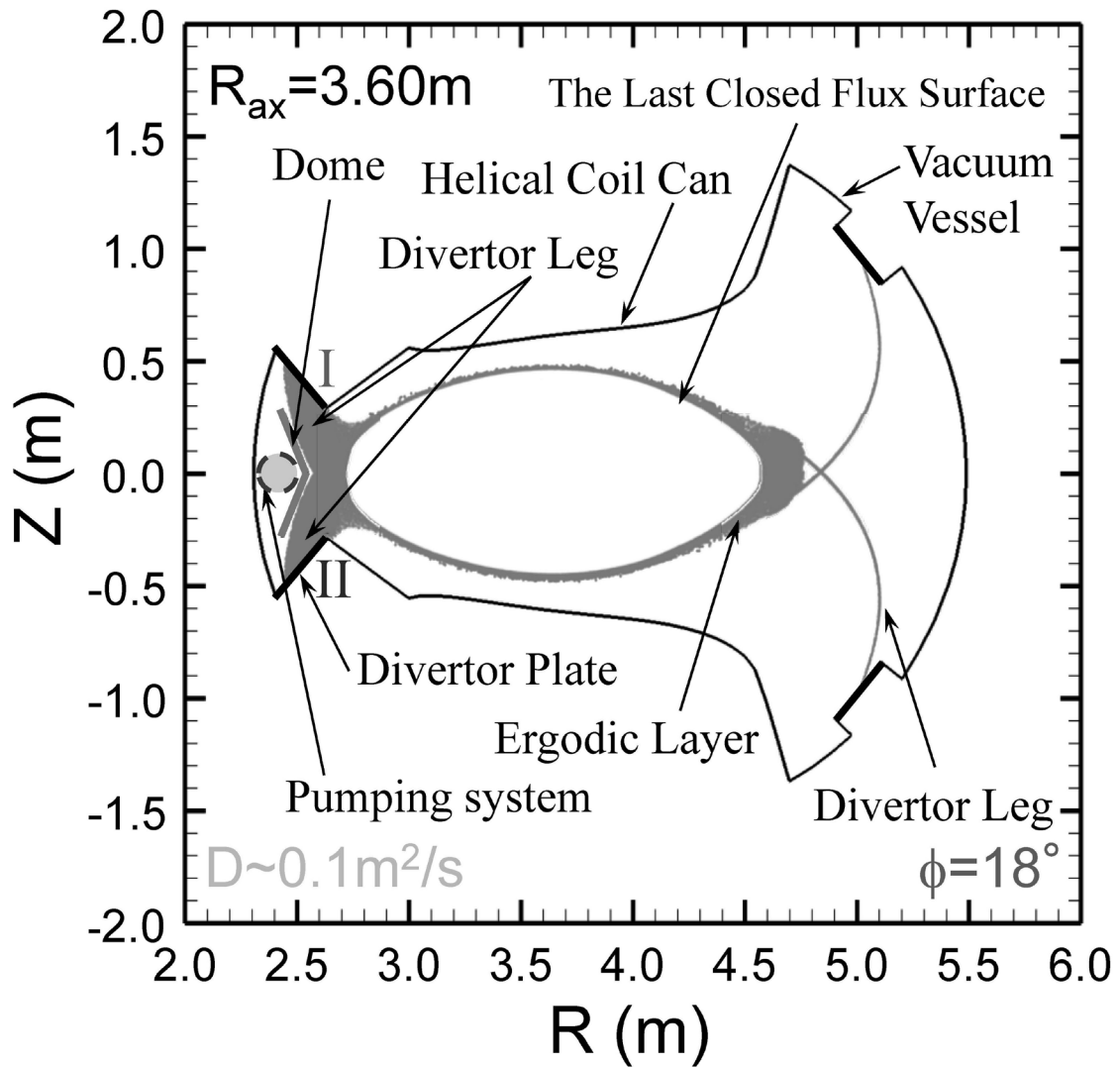EFFICIENT PARTICLE CONTROL IN THE LHD PLASMA PERIPHERY

Fig. 13. M. SHOJI et al., INVESTIGATION OF THE HELICAL DIVERTOR FUNCTION AND THE FUTURE PLAN OF A CLOSED DIVERTOR FOR EFFICIENT PARTICLE CONTROL IN THE LHD PLASMA PERIPHERY
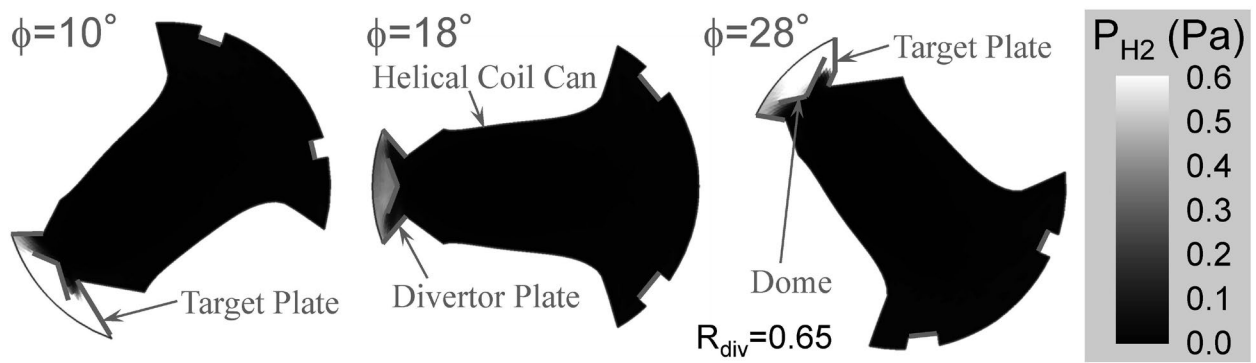
Fig. 14. M. SHOJI et al., INVESTIGATION OF THE HELICAL DIVERTOR FUNCTION AND THE FUTURE PLAN OF A CLOSED DIVERTOR FOR EFFICIENT PARTICLE CONTROL IN THE LHD PLASMA PERIPHERY

REFERENCES

1. N. OHYABU, et al., "Observation of Stable Super Densecore Plasmas in the Large Helical Device", *Phys. Rev. Let.*, **97**, 055002 (2006).

2. O. MOTOJIMA et al., "Overview of Confinement and MHD stability in the Large Helical Device", *Nucl. Fusion*, **45**, S255 (2005).

3. S. MASUZAKI et al., "The divertor plasma characteristics in the Large Helical Device", *Nucl. Fusion*, **42**, 750 (2002).

4. M. GOTO et al., "Spatial distribution measurement of atomic radiation with an astigmatism-corrected Czerny-Turner-type spectrometer in the Large Helical Device", *Rev. Sci. Instr.*, **77**, 10F124 (2006).

5. M. SHOJI et al., "Production of hot spot on a vertically installed divertor plate by ICRF heating in the large helical device", *IEEE Trans. Plasma Sci.*, **33**, 2, 440 (2005).

6. R. KUMAZAWA et al., "Long-pulse plasma discharge on the Large Helical Device", *Nucl. Fusion*, **46**, S13 (2006).

7. Y. FENG et al., "3D Edge Modeling and Island Divertor Physics", *Contrib. Plasma Phys.*, **44**, 57 (2004).

8. K. SAITO et al., "ICRF long-pulse discharge and interaction with a chamber wall and antennas in LHD", *J. Nucl. Mater.*, **363-365**, 1323 (2007).

9. T. WATANABE et al., "Magnetic field structure and confinement of energetic particles in the LHD", *Nucl. Fusion*, **46**, 291 (2006).

10. D. B. HEIFETZ et al., "Monte Carlo Model of Neutral Particle Transport Diverted Plasmas", *J. Comp. Phys.*, **46**, 309 (1982).

11. M. SHOJI et al., "Three-dimensional neutral particle transport simulation for analyzing polarization resolved H-alpha spectra in the large helical device", *J. Nucl. Mater.*, **337-339**, 186 (2005).

12. S. MASUZAKI et al., "Overview and Future Plan of Helical Divertor Study in the Large Helical Device", *Fusion Sci. Technol.*, **50**, 361 (2006).

13. H. OGAWA et al., "Heat- and Particle-Deposition Distribution on Helical Divertor Plates in LHD During Real-Time Magnetic-Axis Swing Operations", *Plasma Fusion Res.*, **2**, 043 (2007).

14. Y. KUBOTA et al., "Design and thermal performance of an improved mechanically attached module for divertor plate of LHD", *Fusion Eng. Des.*, **75-79**, 297 (2005).

15. A. IWAMAE et al., "Polarization resolved H_α spectra from the large helical device: Emission location, temperature, and inward flux of neutral hydrogen", *Phys. Plasmas*, **12**, 042501 (2005).

16. D. REITER et al., "The EIRENE and B2-EIRENE Codes", *Fusion Sci. Technol.*, **47**, 172 (2005).

17. M. SHOJI et al., "Three-dimensional neutral particle transport simulation for analyzing polarization resolved H-alpha spectra in the large helical device", *J. Nucl. Mater.*, **363-365**, 827 (2007).

18. H. YAMADA et al., "Energy confinement and thermal transport characteristics of net current free plasmas in the Large Helical Device", *Nucl. Fusion*, **41**, 901 (2001).

19. M. KOBAYASHI et al., "Analysis for hydrogen particle balance of plasma-wall system in the large helical device", *J. Nucl. Mater.*, **350**, 46 (2006).

20. M. SHOJI et al., "A closed divertor configuration for reduction of the heat load and efficient particle control for helical fusion reactors", *Plasma Fusion Res.*, **3**, S1038

(2008).

21. Y. FENG et al., "Physics of island divertors as highlighted by the example of W7-AS", *Nucl. Fusion*, **46**, 807 (2006).

22. M. KOBAYASHI et al., "Impurity retention effect in the edge ergodic layer of LHD", *Plasma Fusion Res.*, **3**, S1005 (2008).